Hindawi
Advances in Civil Engineering
Volume 2019, Article ID 6380815, 14 pages
https://doi.org/10.1155/2019/6380815

Research Article

Three-Dimensional Analysis of Complex Rock Slope Stability Affected by Fault and Weak Layer Based on FESRM

Yang Li[1,2], **Ling Yu**[3], **Weidong Song**[1,2] **and Tianhong Yang**[4]

[1]*Key Laboratory of Ministry of Education for Efficient Mining and Safety of Metal Mines, University of Science and Technology Beijing, Beijing 100083, China*
[2]*School of Civil and Resource Engineering, University of Science and Technology Beijing, Beijing 100083, China*
[3]*Institute of Opencast Mining Safety, CCTEG Shenyang Research Institute, Fushun, Liaoning 113122, China*
[4]*School of Resources and Civil Engineering, Northeastern University, Shenyang, Liaoning 110819, China*

Correspondence should be addressed to Yang Li; leon.42@163.com and Ling Yu; yuling1214@qq.com

Received 15 August 2019; Revised 11 October 2019; Accepted 31 October 2019; Published 7 December 2019

Academic Editor: Rafael J. Bergillos

Slope stability analysis is the most important problem in slope engineering design and construction. Open-pit slope often spans several strata, many of which are relatively weak. There may be faults and weak layers across the whole rock. It is very necessary to study the instability mechanism and stability analysis of multistratigraphic slopes with faults and weak layers. In this paper, taking a complex three-dimensional slope with fault and weak layer as the research object, the evolution laws of the stress field and damage zone of the slope are analyzed by using the finite element strength reduction method. The results show that the fault and weak layer have different degrees of effect on the slope stability. The fault causes stress concentration and damage to nearby rock mass, and the weak layer causes stress concentration on the slope above it and forms a dangerous slip zone. Then the effect of the fault and weak layer on slope stability is discussed. Because the effect of horizontal structural plane on slope stability is greater than that of the vertical structural plane, the effect of weak layer on slope stability is greater than that of the fault in the slope. The research results can provide a theoretical guidance for the study of slope stability in practical engineering.

1. Introduction

As the starting point of all slope engineering designs, slope stability analysis has become the most important problem in slope engineering, and it has also attracted the attention of the industry as one of the most difficult problems in slope engineering design and construction. The main task of slope stability analysis is calculating the stability and evaluating its stability state and deformation trend [1, 2]. Open-pit mine slopes are usually excavated on natural rock masses. These rock masses are the product of long-term geological development. They are generally divided by various geological interfaces in varying degrees, which makes the rock mass to have complex discontinuous features. Open-pit mine slopes often span several strata, many of which are relatively weak, because there may be faults that traverse the whole rock and soil. A serious problem for the study of open-pit slopes is put forward: the instability mechanism and stability analysis of multistratigraphic slopes with faults and weak layers.

Two-dimensional (2D) analysis of slopes is a common method. However, the traditional 2D calculation method makes assumptions on the interstrip force and slip surface. The analysis result is only the stability state of a section, which can only reflect the local stability of the slope. Most of the disasters such as slope landslides that occur in the practical engineering show the three-dimensional (3D) state. If the traditional 2D analysis method is used under complex geological conditions, the analysis results will be quite different from the actual situation. But 3D slope stability analysis can more realistically reflect the actual situation of the slope [3]. With the development of computer technology, more and more researchers are now using the 3D finite

element method (FEM) to study the stability of slopes. By using 3D FEM, the safety factor of the slope can be calculated [4–6], the safety assessment of the dangerous area can be carried out [7–9], and the failure mode and mechanism of the slope can be studied [10–12].

The strength reduction elastoplastic finite element numerical analysis method was first put forward by Zienkiewicz et al. [13] in 1975. Ugai's research made the finite element strength reduction method (FESRM) to begin to attract attention from the academic community in slope stability analysis in 1989 [14]. And it is proposed that the elastoplastic finite element strength reduction method is an adaptive and feasible slope stability analysis method. Griffiths and Lane [15], Dawson et al. [16], Manzari and Nour [17], and Tschuchnigg et al. [18] have applied the FESRM to the slope stability analysis. The safety factor calculated by using FESRM has many advantages over the conventional method [19–21]. There is no need to artificially assume the position of the slip surface, which is suitable for the stability analysis of complex slopes. Especially when there are faults and weak layers in the slope, it can better reflect its advantages [22–26]. According to the information of stress field and strain field obtained by finite element calculation, the failure process of slope can be dynamically simulated, that is, the process of occurrence, development, and yield failure of slope can be described. Thus the failure mode, the characteristics of stress and the mechanism of damage evolution of complex slopes can be analyzed. Therefore, FESRM is an effective means to calculate and analyze the stability of complex slopes.

A number of researchers have carried out related research on the slope stability analysis under the effect of faults or weak layers, and many meaningful results have been achieved. But there are few studies on the stability of 3D slope under the control of faults and weak layers. In this paper, the open-pit slope with fault and weak layer is taken as the research object. Based on FESRM, the rock slope is analyzed by the finite element analysis software COMSOL Multiphysics. The stress evolution and damage mechanism of the slope affected by the fault and weak layer are studied. The comparative analysis under different conditions is carried out, revealing the role played by fault and weak layer in slope instability. The research results can provide a theoretical basis for the study of slope deformation and damage in practical engineering.

2. Geomining Conditions

The open-pit mine stratum structure and engineering geological conditions are complex. The strata in the mining area are metamorphic rocks. Due to the different composition and metamorphism of the parent rock, the hardness of the rock layers is different. In the vertical direction, weak and hard interlayers appear, and in the horizontal direction, it appears as weak and hard in the same rock stratum. Therefore, the lithology of the stratum is different, the mechanical strength of the rock is low, and the stability of the whole slope is poor.

The 3D rock slope studied in this paper is located in the east of the mining area. The slope inclination is 230°, the highest slope height is 330 m, and the slope angle is 30°. The slope contains 10 groups of geological rock groups (as shown in Table 1). From top to bottom, they are Q (quaternary topsoil), fault F1 (embedded in the slope), CMN (clay talc dolomite, dolomitic siltstone, and dolomitic sandstone), SDS (light yellow dolomitic shale and dolomite), weak layer BOMZ (quartz sandstone), SDB (shallow white dolomitic shale), RSC1 (massive and honeycomb silicified dolomite), RSC2 (massive and honeycomb silicified dolomite), RSF (layered silicified dolomite), and RAT (dolomitic siltstone). The rock mass structure of the slope is very complicated. Slope rock mass is layered distribution, in which the rock mass above 1250 m is loose structure and its shape is soil-like and fragmentary; the rock mass between 1250 m and 1200 m is fragmented structure, and its shape is sandy and fragmentary; and the rock mass between 1200 m and 1100 m is massive structure, and its shape is columnar and long columnar. There is a fault F1 in the slope, which is going to NE15~20°, tending SE, and the inclination angle is 20°. The surface exposure length of the fault is about 450 m, and the width is 10~20 m. The small folds, fault scratches, schistosome zone, and tectonic breccia are visible in the fault. There is a BOMZ weak layer which is layered loose rock mass. It is loose structure, and its strength is low.

3. Model Building

The slope shape is irregular, and the contact relationship between rock strata is very complex in practical engineering. In order to establish a 3D model for finite element analysis, it is necessary to simplify it properly to ensure that the model can be calculated successfully.

(1) The rock mass of each stratum is regarded as a unified lithology, and the model does not specifically reflect the joints, fissures, and composition of rock mass. It is reflected by its corresponding parameters (including elastic modulus, Poisson's ratio, cohesion, and internal friction angle).

(2) In fact, the slope has been excavated, showing a stepped shape. At the same time, the occurrence of rock and fault planes is irregular. However, in order to facilitate the establishment of a 3D model, it is assumed that the slope surface is smooth from the top to the bottom of the slope and that the rock and fault planes are also smooth.

Based on the above two assumptions, a 3D slope model was built by 3D mining software, as shown in Figure 1. The geometry of the model is 1000 m × 450 m × 600 m, of which the slope height is 300 m.

In order to demonstrate the formation occurrence of the slope model, the exploded view of the 3D slope model was established, as shown in Figure 2. The occurrence of the fault and weak layer in the slope can be clearly identified.

The boundary condition is that the upper surface is free, the surrounding is constrained by normal displacement, and

Table 1: Physico-mechanical parameters of the 3D model.

Stratum	Density ρ (g/cm^3)	Cohesion c (kPa)	Internal friction angle φ (°)	Elastic modulus E (GPa)	Poisson's ratio μ
Q	19.4	38.2	23.2	0.02	0.38
CMN	21.2	130	27.6	1.5	0.25
Fault F1	17.6	10	20	0.08	0.35
SDS	22.6	248	29.8	2.0	0.203
BOMZ (weak layer)	19.4	120	27.6	0.54	0.22
SDB	23.5	340	33.8	2.5	0.209
RSC1	24.2	600	36	3.0	0.209
RSC2	19.5	600	30	1.0	0.203
RSF	24.3	860	40.2	4.0	0.205
RAT	27.3	880	46	10	0.21

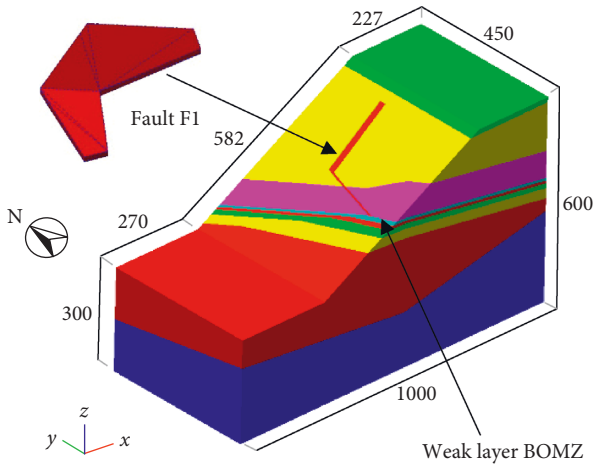

Figure 1: Three-dimensional slope model.

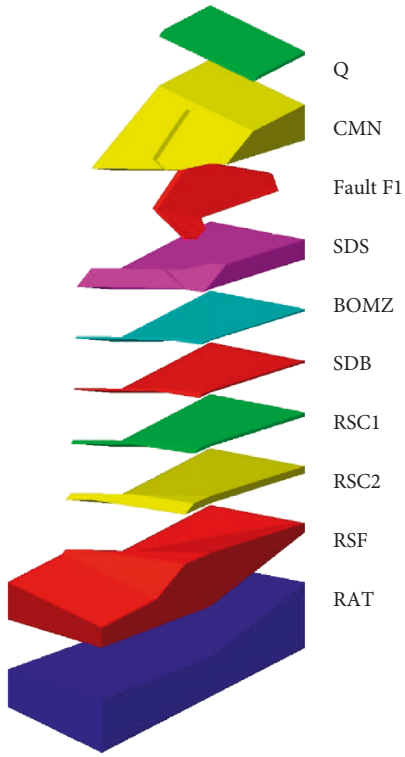

Figure 2: Exploded view of the 3D slope model.

the bottom surface is fixed. The model is only subjected to self-weight, and free settlement is allowed.

The model is divided into 10 layers (Q layer to RAT layer from top to bottom, see Figure 2). The mechanical parameters of each layer are shown in Table 1. The mechanical parameters of the 3D model are obtained by the Hoek–Brown criterion. According to rock mechanical test results and engineering geology and hydrogeology characteristics, combined with rock mass characteristics of the slope, the rock physical and mechanical parameters can be determined. Firstly, the mechanical parameters of rock samples are obtained through laboratory tests. Due to the natural characteristics, there are many factors that impact mechanical parameters of slope rock mass, such as structural plane and groundwater storage. So, using rock quality classification indices, the value of RMR (rock mass rating) [27] can be obtained. Then according to the RMR value, the rock mass parameters are calculated based on the Hoek–Brown criterion [28–31]. Finally, the rock mass parameters are synthetically determined considering the results of rock mass quality classification.

Because the selection of fault mechanical parameters lacks empirical formulas, the mechanical parameters of the fault in the manuscript are determined by experience analogy. The selected mechanical parameters of the fault are the peak strength. Because there is no reliable theoretical basis for experience analogy, in order to determine the rationality of experience analogy fault parameters, the parameters in four cases are selected for comparison and discussion. The following are the four cases: (1) experience analogy parameters; (2) lower than experience analogy parameters; (3) higher than experience analogy parameters; and (4) the same as weak layer mechanical parameters. The calculation results are shown in Figure 3. It can be seen that the stress distribution characteristics of the calculated results in the four cases are basically the same, but the numerical values are just different. The second case can also be regarded as the residual strength of the fault. Even if residual strength is selected, the failure mode of the slope is basically unchanged. That is to say, the failure mode of the slope is mainly controlled by structure (the weak layer), and the mechanical parameters of fault have little effect on it. This paper studies the slope stability under the effect of the fault and weak layer. The main concern is the mode of slope deformation and failure, while the mechanical parameters of

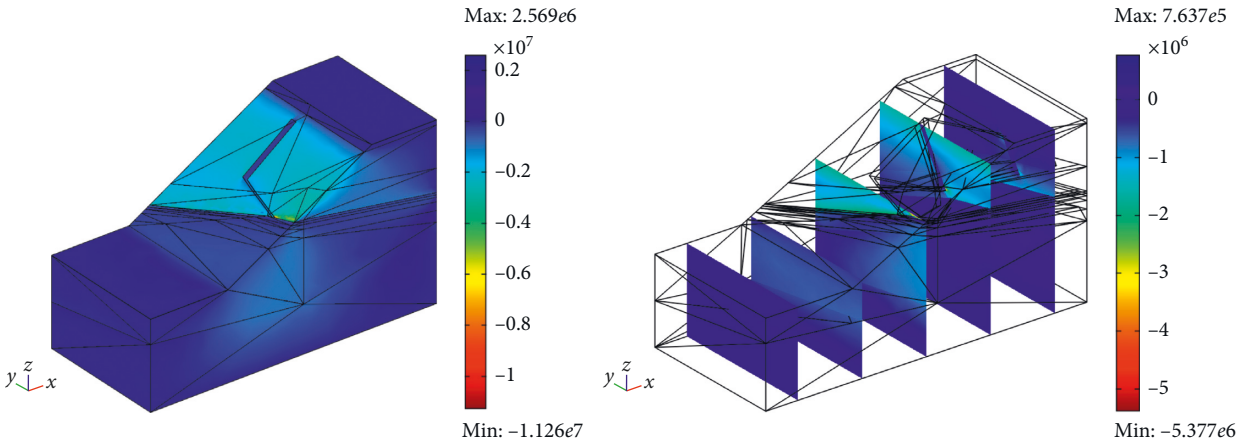

(a)

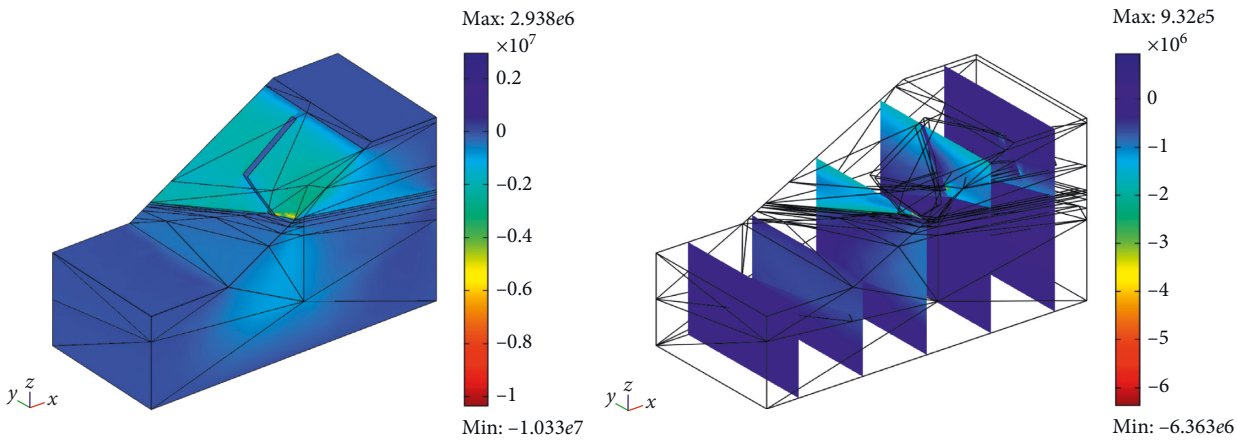

(b)

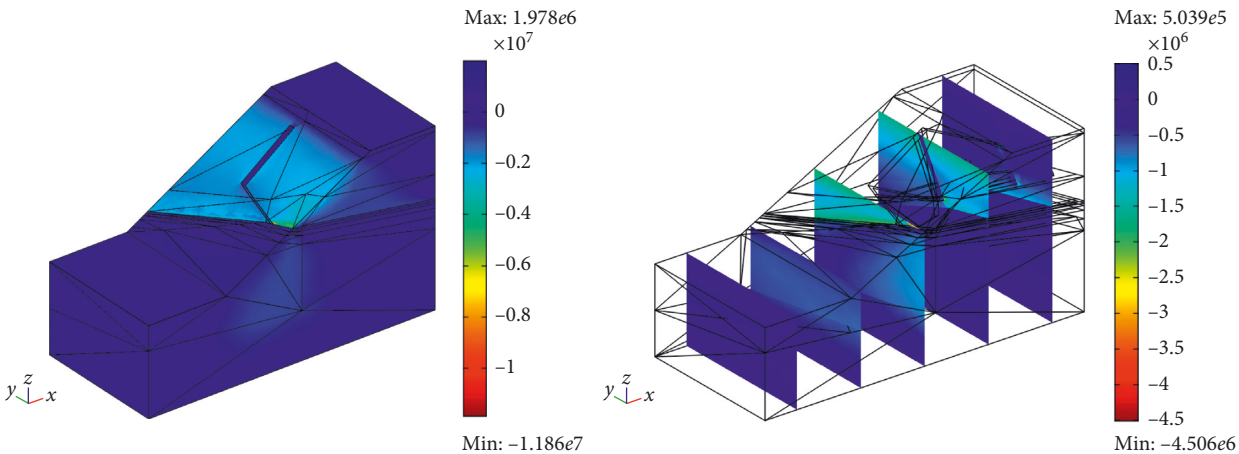

(c)

Figure 3: Continued.

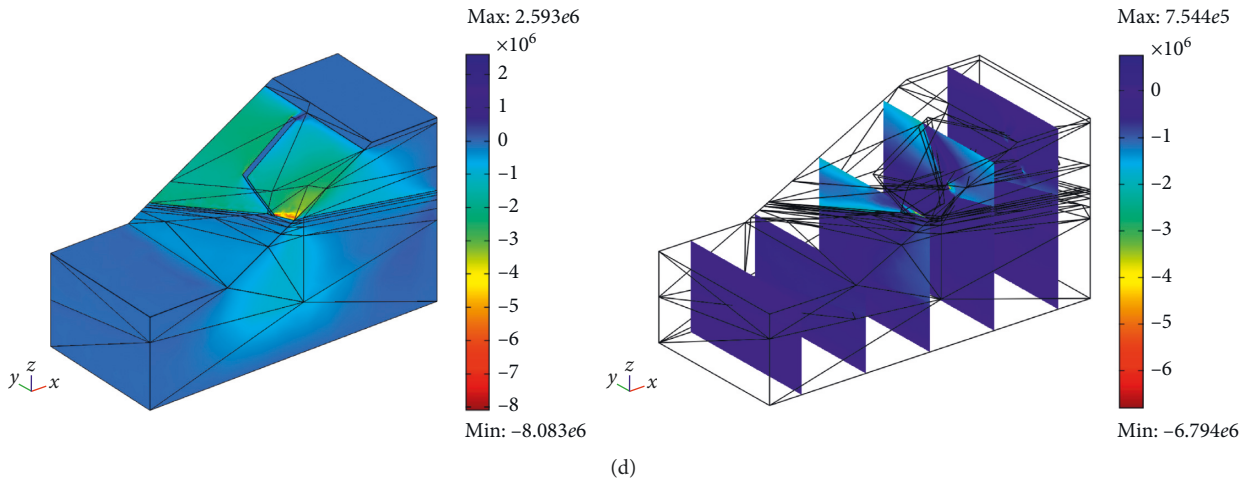

(d)

FIGURE 3: The calculation results in the four cases: (a) experience analogy parameters; (b) lower than experience analogy parameters; (c) higher than experience analogy parameters; (d) the same as weak layer mechanical parameters.

the fault have little effect on the mode of slope failure, so it is acceptable to determine the fault parameters by experience analogy.

4. Calculation Method

4.1. Strength Reduction Method. Zienkiewicz et al. first proposed the concept of the shear strength reduction factor in finite element numerical analysis [13]. The shear strength reduction factor is the ratio of the maximum shear strength formed by the slope soil and the actual shear stress caused by the external load under the continuous external load. The principle is simply summarized as follows: the shear strength parameters of slope soil are reduced by continuous reduction, and the reduced parameters are replaced by repeated calculation of the model until the model is calculated to the ultimate failure. The formula of the strength reduction method is as follows:

$$\begin{aligned} c' &= \frac{c}{F}, \\ \tan\varphi' &= \frac{\tan\varphi}{F}, \end{aligned} \tag{1}$$

where cohesion c and internal friction angle φ are the strength parameters of rock and soil before reduction; c' and φ' are the actual strength parameters of rock and soil after reduction; and F is the strength reduction factor of rock and soil mass.

4.2. Yield Criterion. The constitutive model of geomaterials in FESRM usually adopts the ideal elastoplastic model. The yield criterion generally selects the Drucker–Prager (D-P) criterion [32, 33], which accounts for the effect of the intermediate principal stress, and considers the effect of hydrostatic pressure. So, the D-P criterion overcomes the main weakness of the Mohr–Coulomb criterion. The D-P criterion is extended and promoted based on the Mohr–Coulomb criterion and the von Mises criterion in elastoplastic mechanics:

$$f = \alpha I_1 + \sqrt{J_2} - K = 0, \tag{2}$$

where I_1 is the first invariant of stress and represented by the following equation:

$$I_1 = \sigma_{ii} = \sigma_1 + \sigma_2 + \sigma_3 = \sigma_x + \sigma_y + \sigma_z, \tag{3}$$

and J_2 is the second invariant of the stress deviator and represented by the following equation:

$$\begin{aligned} J_2 &= \frac{1}{6}\left[(\sigma_1 - \sigma_2)^2 + (\sigma_2 - \sigma_3)^2 + (\sigma_3 - \sigma_1)^2\right] \\ &= \frac{1}{6}\Big[(\sigma_x - \sigma_y)^2 + (\sigma_y - \sigma_z)^2 + (\sigma_z - \sigma_y)^2 \\ &\quad + 6\left(\tau_{xy}^2 + \tau_{yz}^2 + \tau_{zx}^2\right)\Big], \end{aligned} \tag{4}$$

where α and K are the experimental constants related only to the internal friction angle φ and the cohesion c of the rock:

$$\begin{aligned} \alpha &= \frac{2\sin\varphi}{\sqrt{3}(3 - \sin\varphi)}, \\ K &= \frac{6c\cos\varphi}{\sqrt{3}(3 - \sin\varphi)}. \end{aligned} \tag{5}$$

5. Results and Analysis

Based on the 3D mechanical model, the COMSOL Multiphysics system was used to solve the large-scale stress field calculation and analysis. The system is a multiphysics-coupled process analysis tool developed based on partial differential equations (PDEs), which can be solved by an efficient solver based on FEM.

5.1. Shear Stress Analysis. Figure 4(a) shows the shear stress field on the *xz* plane of the slope. The shear stress is concentrated along the slope above the weak layer BOMZ, and the concentrated area is divided into two parts by the fault F1. Because the fault is not completely vertical but tortuous, the stress concentration is not obvious in the south of the fault but high in the north, especially in the area close to the fault. The maximum stress value occurs at the junction of the end of the fault and weak layer. Damage is easy to occur in the area where shear stress is concentrated. In the future, it is necessary to strengthen the monitoring to prevent landslides. Figure 4(b) is the sectional view of the shear stress field. It can be clearly seen that the stress concentration in the slope caused by the weak layer and the stress distribution in the slope are more complex because of the existence of the fault. The structural planes like fault and weak layer act as barriers for stress concentration [34, 35].

5.2. Principal Stress Vector Analysis. Figure 5 shows the principal stress vector diagram of the slope model. The simulation arrows of $8 \times 5 \times 5$ principal stress vectors are set in the directions of *x*, *y*, and *z*, respectively. Under the effect of the self-weight of the slope, the size of the vector arrow from bottom to top decreases gradually. The fault F1 is embedded in the slope and exposed along the slope surface, which has a certain influence on the distribution of the principal stress vector. According to the mechanical parameters of each stratum, the elastic moduli of the weak layer and the fault are only 0.08 GPa and 0.54 GPa, respectively, while that of CMN on both sides of the fault is 1.5 GPa. The strength of rock mass varies greatly among these strata. In addition, the normal displacement around the slope model is constrained, so the principal stress vector will move towards the lower strength strata. The principal stress vectors on both sides of the fault and weak layer deflect along the strike of them. Therefore, it can be judged that under the effect of the fault and weak layer, the area along both sides of the fault and weak layer will be the first area where damage occurs.

5.3. Damage Zone Analysis. The damage zone of the slope is calculated by using the D-P criterion and FESRM. Figure 6 shows the evolution of the damage zone, and for Figures 6(a)–6(d), strength reduction factors of 1.00, 1.30, 1.70 and 2.00 are selected, respectively. It can be seen that the fault and weak layer first produce damage. With the strength of rock mass decreasing, the damage area along the fault and weak layer gradually expands and eventually extends to the whole slope surface. Comparing with the shear stress field in Figure 4, it shows that the damage of the slope is mainly caused by shear stress. However, there is almost no damage zone in the rock mass below the weak layer, which further illustrates the control role of the weak layer in slope failure. Figure 7 is the sectional view of damage zone development. It can be seen that the damage originates at the fault and weak layer and gradually extends to a large area with the strength reduction. Finally, a complete slope slip zone is formed.

6. Discussion

The previous calculation results and analysis are based on the interaction of the fault and weak layer. In order to analyze the effect of the fault and weak layer on slope stability separately, the calculation model is changed to that include only fault or weak layer. Then the change laws of the stress field and damage zone are analyzed.

6.1. Effect of Fault. The 3D slope model with fault and weak layer is modified. The strength parameter of weak layer BOMZ is modified to that of SDS. Then, the 3D slope model with fault is obtained. The result is analyzed by the same calculation method and strength criteria.

6.1.1. Stress Field. Figure 8 is the shear stress field on the *xz* plane of the slope with fault. Without the barrier of the weak layer, the shear stress is mainly concentrated on the whole slope surface, especially the rock mass near the fault and below the slope. Due to the effect of the self-weight load of the strata and the normal restraint on both sides, a stress concentration zone is formed in the boundary area between RSF and RAT below the slope. Although it is the stress concentration area, there is no danger of damage because of its deep location and the high strength of the strata. It can be seen from Figure 8(b) that the shear stress distribution near the fault is not uniform due to the existence of the fault. But the strength of the fault is low, so it is easy to cause rock damage here.

Figure 9 shows the principal stress vectors of the slope with fault. The simulation arrows of $8 \times 5 \times 5$ principal stress vectors are set in the directions of *x*, *y*, and *z*, respectively. Because the strength of the fault is quite different from that of surrounding rock mass and four sides of the slope model are constrained normal displacement, the principal stress vector will move towards the fault. The principal stress vectors on both sides of the fault slightly deflect along the strike of the fault. It can be judged that, under the effect of the fault, both sides of the fault will become the first area where the damage occurs.

6.1.2. Damage Zone. Figure 10 shows the evolution of the damage zone of the slope with fault. When $F = 1.0$, only a small amount of damage is generated at the fault. As the strength of the rock mass decreases, the damage of the rock mass gradually extends from the fault to the slope on both sides of it. However, the damage area of the slope with fault is smaller than that of the slope with fault and weak layer. The stratum of the slope is low in the north and high in the south. The strata on the south side show antidip geological structure, while the strata on the north side show a trend of transformation to forward dip geological structure. Therefore, the damage development of the south side is slower than that of the north side of the slope. From the sectional view of the damage zone (Figure 11), it can be seen that the damage occurs at the bend of the fault first, extends to the upper strata and deep part of the fault, and then forms a slip

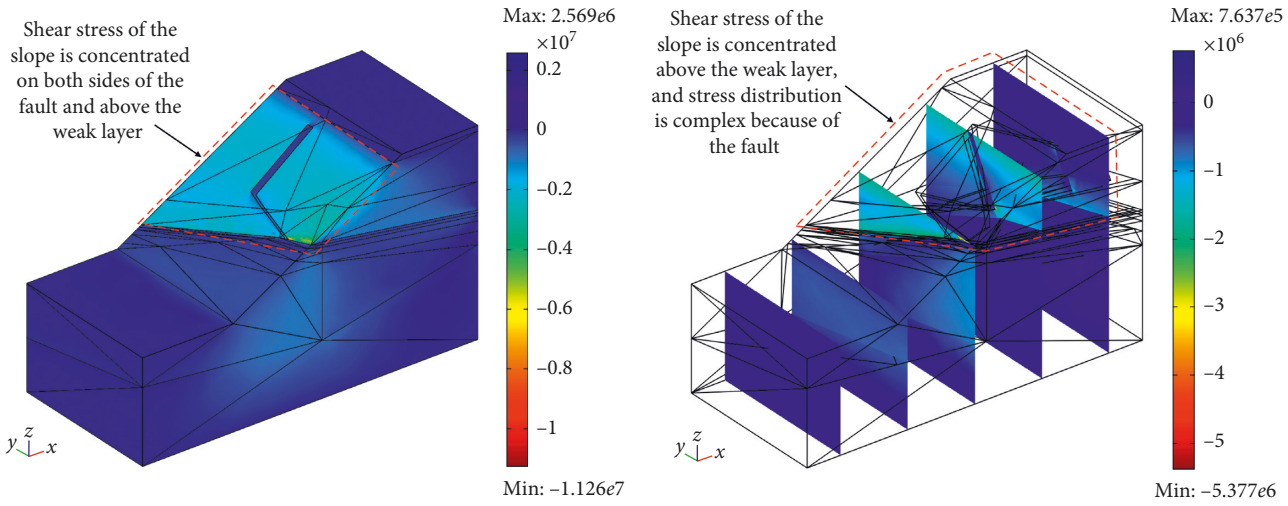

Figure 4: Shear stress field on the *xz* plane. (a) 3D view. (b) Sectional view.

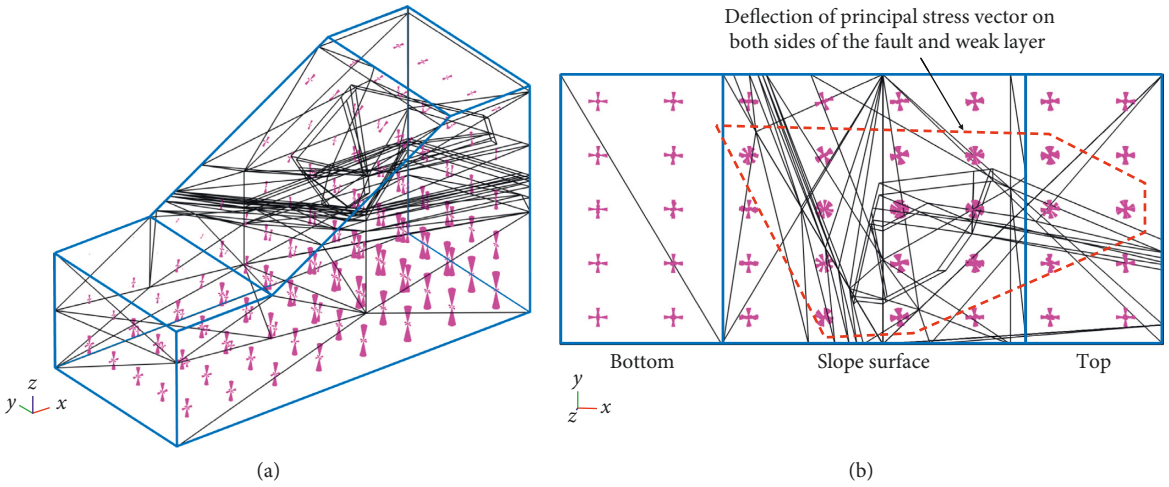

Figure 5: The principal stress vector diagram. (a) 3D view. (b) Top view.

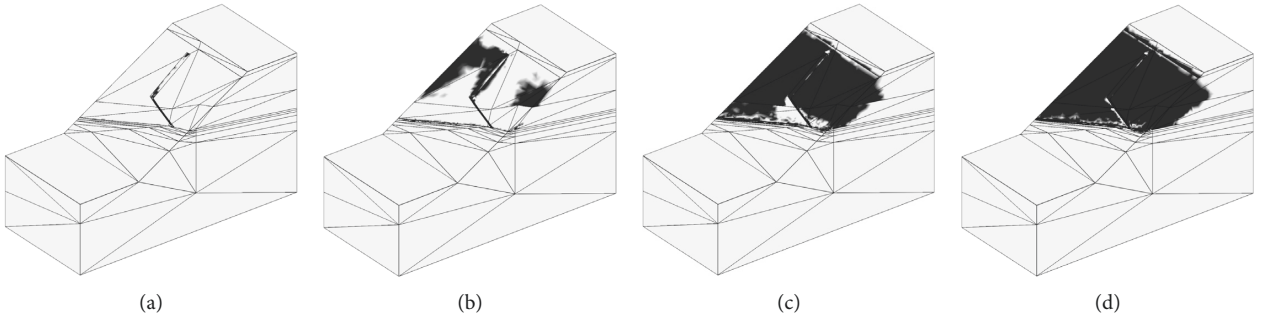

Figure 6: Evolution of the damage zone. (a) $F = 1.0$; (b) $F = 1.3$; (c) $F = 1.7$; (d) $F = 2.0$.

zone with increase of the strength reduction factor. However, the range of the slip zone of the slope with fault is smaller than that of the slope with both fault and weak layer.

6.2. Effect of Weak Layer. Using the slope model in Section 3, the fault F1 is removed and a 3D slope model with weak layer is established, as shown in Figure 12. The results are analyzed using the same calculation method and strength criteria.

6.2.1. Stress Field. Figure 13 is the shear stress field of the slope with weak layer on the *xz* plane. It can be seen that

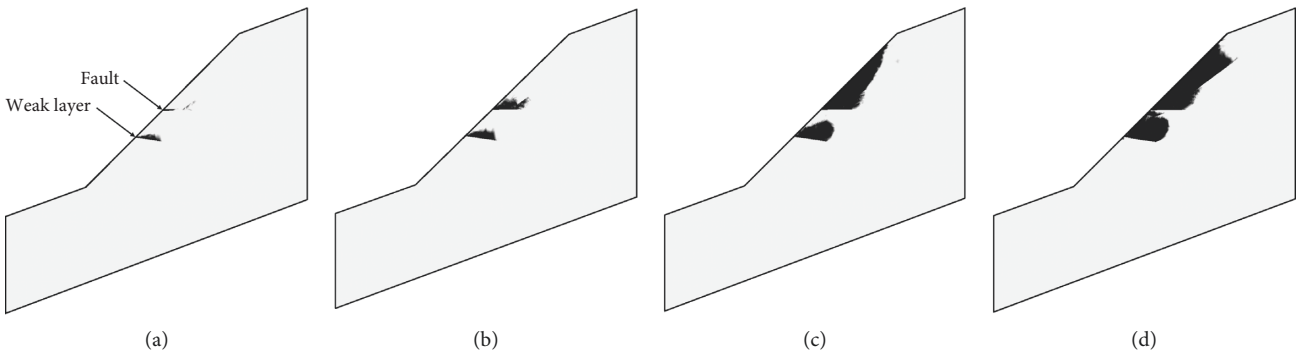

Figure 7: Sectional view of the damage zone. (a) $F = 1.0$; (b) $F = 1.3$; (c) $F = 1.7$; (d) $F = 2.0$.

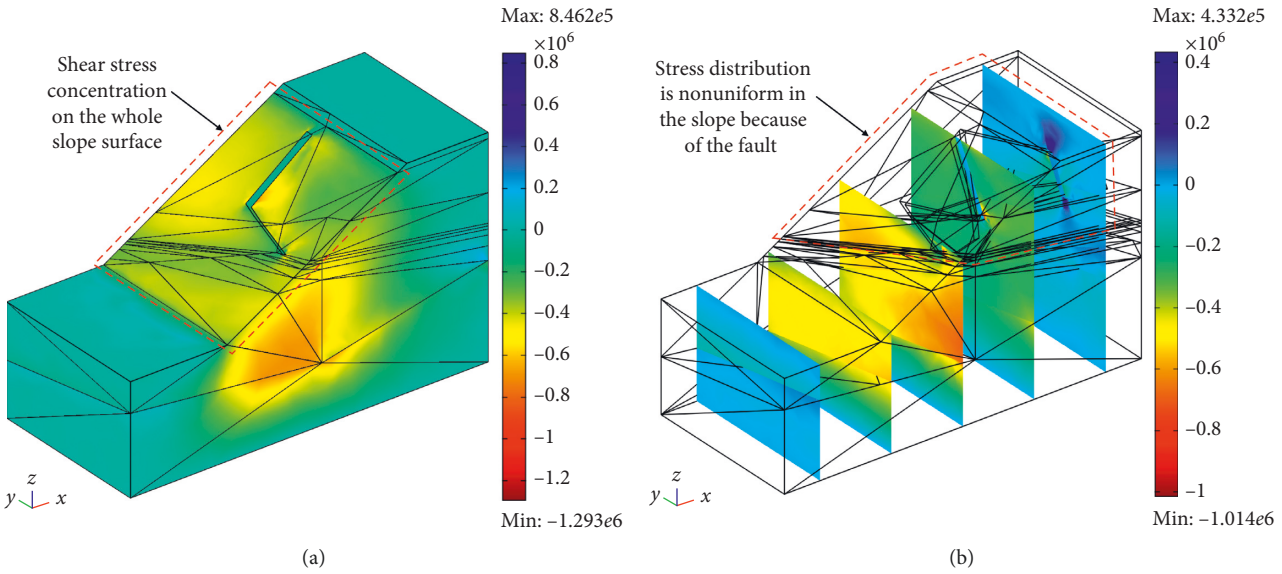

Figure 8: Shear stress field of the slope with fault on the xz plane. (a) 3D view. (b) Sectional view.

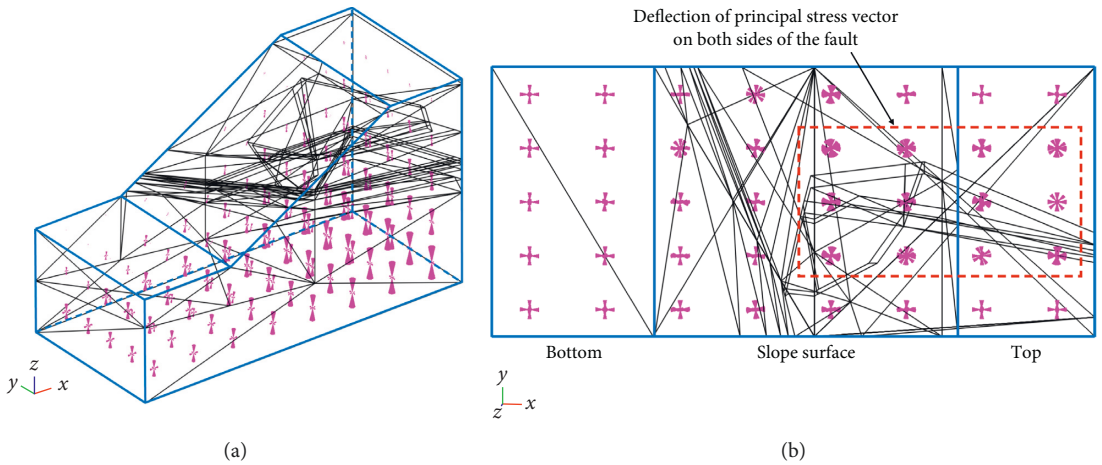

Figure 9: The principal stress vectors of the slope with fault. (a) 3D view. (b) Top view.

the shear stress concentration zone is above the weak layer and the maximum shear stress value appears at the southern part of the junction of the weak layer and SDS, indicating the control effect of the weak layer on the slope stability. As shown in Figure 13(b), the shear stress concentration zone in the slope also appears in the rock

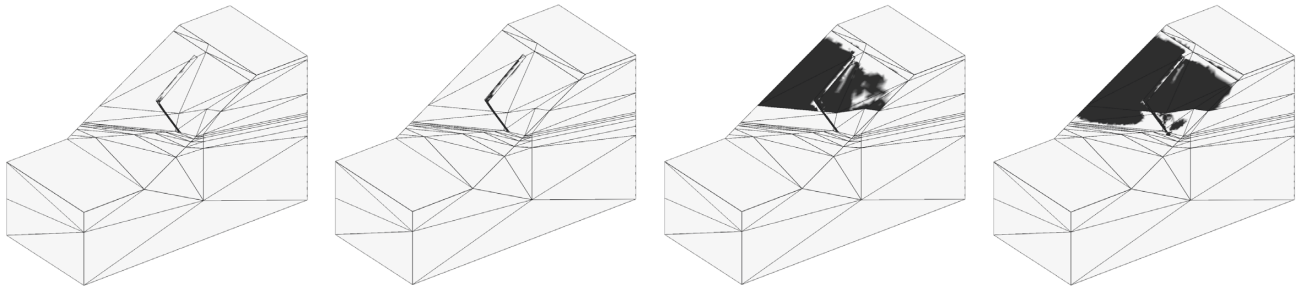

Figure 10: Evolution of the damage zone of the slope with fault. (a) $F = 1.0$. (b) $F = 1.3$. (c) $F = 1.7$. (d) $F = 2.0$.

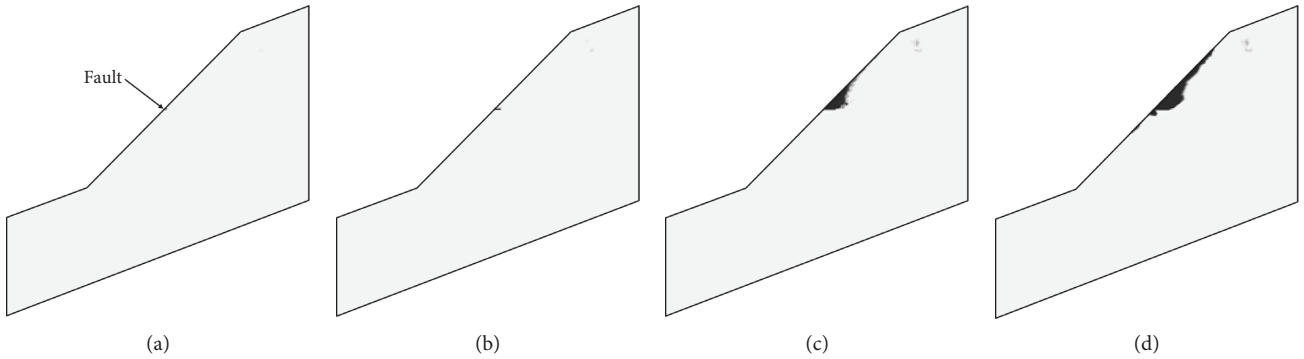

Figure 11: Sectional view of the damage zone of the slope with fault. (a) $F = 1.0$. (b) $F = 1.3$. (c) $F = 1.7$. (d) $F = 2.0$.

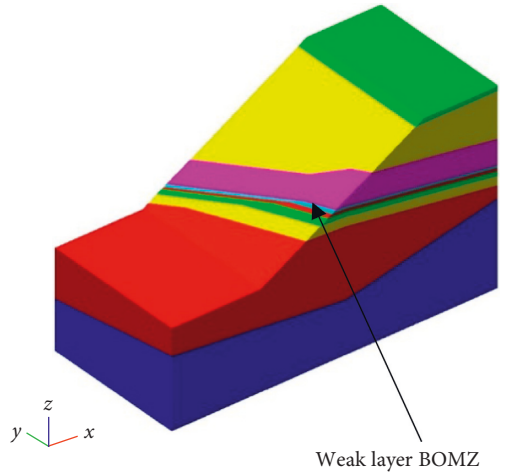

Figure 12: The slope model with only weak layer.

mass above the weak layer. And because there is no fault, the stress distribution is more uniform.

Figure 14shows the principal stress vector of the slope with weak layer. In the model, simulated arrows of $8 \times 5 \times 5$ principal stress vectors are set in the x, y, and z directions, respectively. Due to the large difference in strength between the weak layer and the surrounding rock mass, the principal stress vector will move towards the weak layer. The directions of the principal stress vectors on both sides of the weak layer deflect along the strike of the weak layer. So under the effect of the weak layer, the slope near it will damage firstly.

6.2.2. Damage Zone. Figure 15 shows the evolution of the damage zone of the slope with weak layer. When $F = 1.0$, the damage occurs near the weak layer. As the strength reduction factor increases to 1.3, CMN damages in the shallow part of the slope. When the strength reduction factor increases to 1.7 and 2.0, the damage zone gradually extends to the slope surface above the weak layer. Figure 16 is the sectional view showing the development of the damage zone. In the process of development from $F = 1.0$ to 1.3, the first damage occurred is the weak layer, and the damage gradually extends to the inside of the slope. With the increase of the strength reduction factor, the damage zone extends to the rock mass above the weak layer, forming a complete slip zone.

6.3. Comparative Analysis. The stress field and damage zone under the three conditions (the conditions of only fault, only weak layer, and both fault and weak layer) are compared and analyzed to obtain the effect of the fault and weak layer on the slope stability.

6.3.1. Comparative Analysis of Stress Field. Figure 17 shows the shear stress field on the xz plane under three conditions. When the slope contains only fault, shear stress concentration is generated in the surrounding rock mass of the fault due to its low strength. When the slope contains only weak layer, a large range of shear stress concentrations are generated in the rock mass above the weak layer. When the slope contains the fault and weak layer, the shear stress

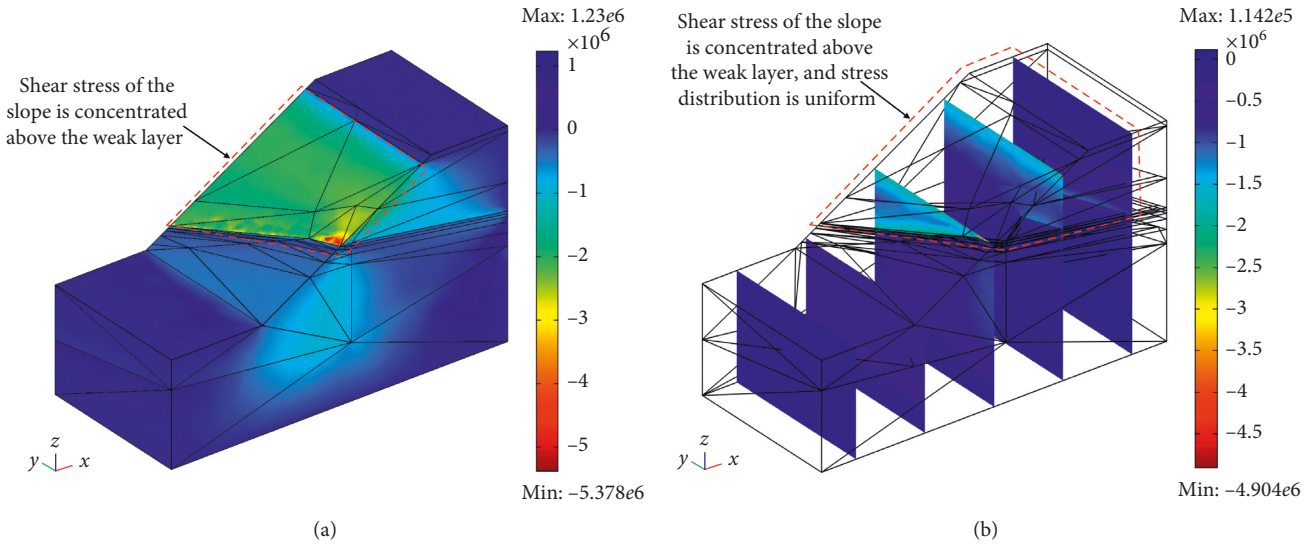

Figure 13: Shear stress field of the slope with weak layer on the *xz* plane. (a) 3D view. (b) Sectional view.

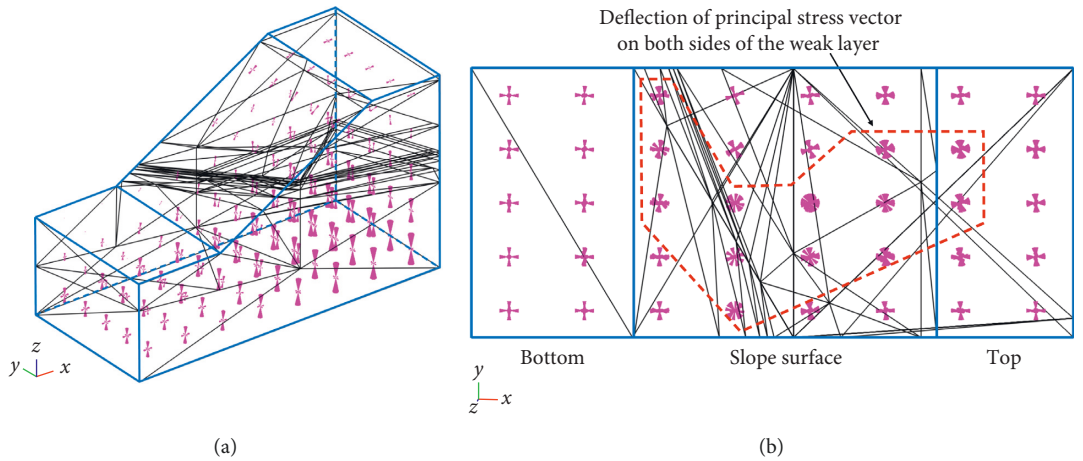

Figure 14: The principal stress vectors of the slope with weak layer. (a) 3D view. (b) Top view.

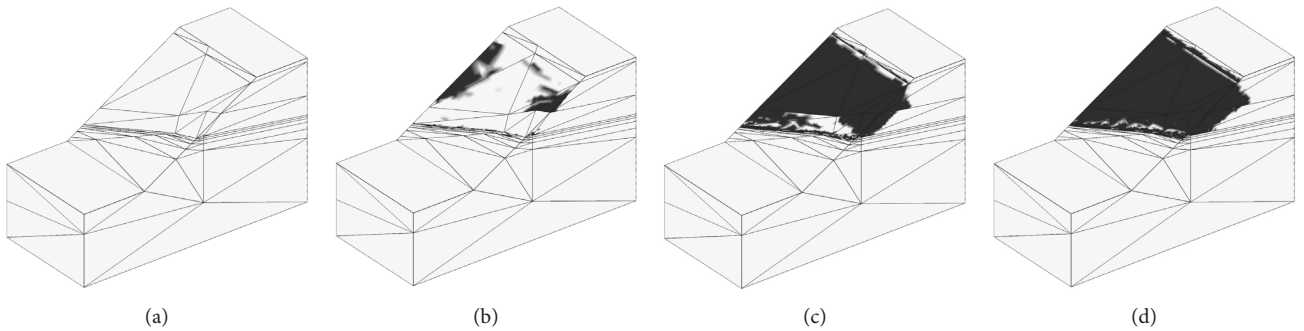

Figure 15: Evolution of the damage zone of the slope with weak layer. (a) $F = 1.0$. (b) $F = 1.3$. (c) $F = 1.7$. (d) $F = 2.0$.

concentration zone is also mainly generated in the rock mass above the weak layer. But the stress distribution inside the rock mass is more complicated because of the effect of the fault.

In order to compare and analyze the numerical changes of the stress field under the three conditions, a data extraction line parallel to the slope is set at the vertical depth of 2 m on the slope surface. Figure 18 shows the variation of

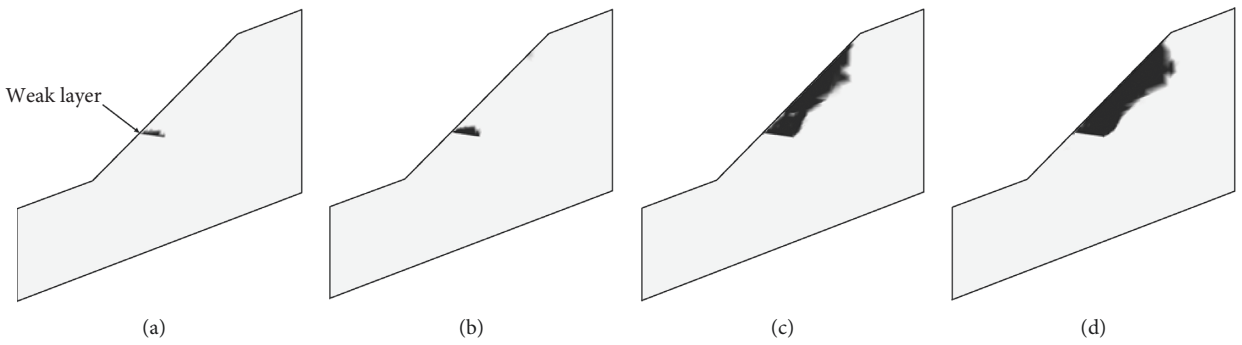

Figure 16: Sectional view of the damage zone of the slope with weak layer. (a) $F = 1.0$. (b) $F = 1.3$. (c) $F = 1.7$. (d) $F = 2.0$.

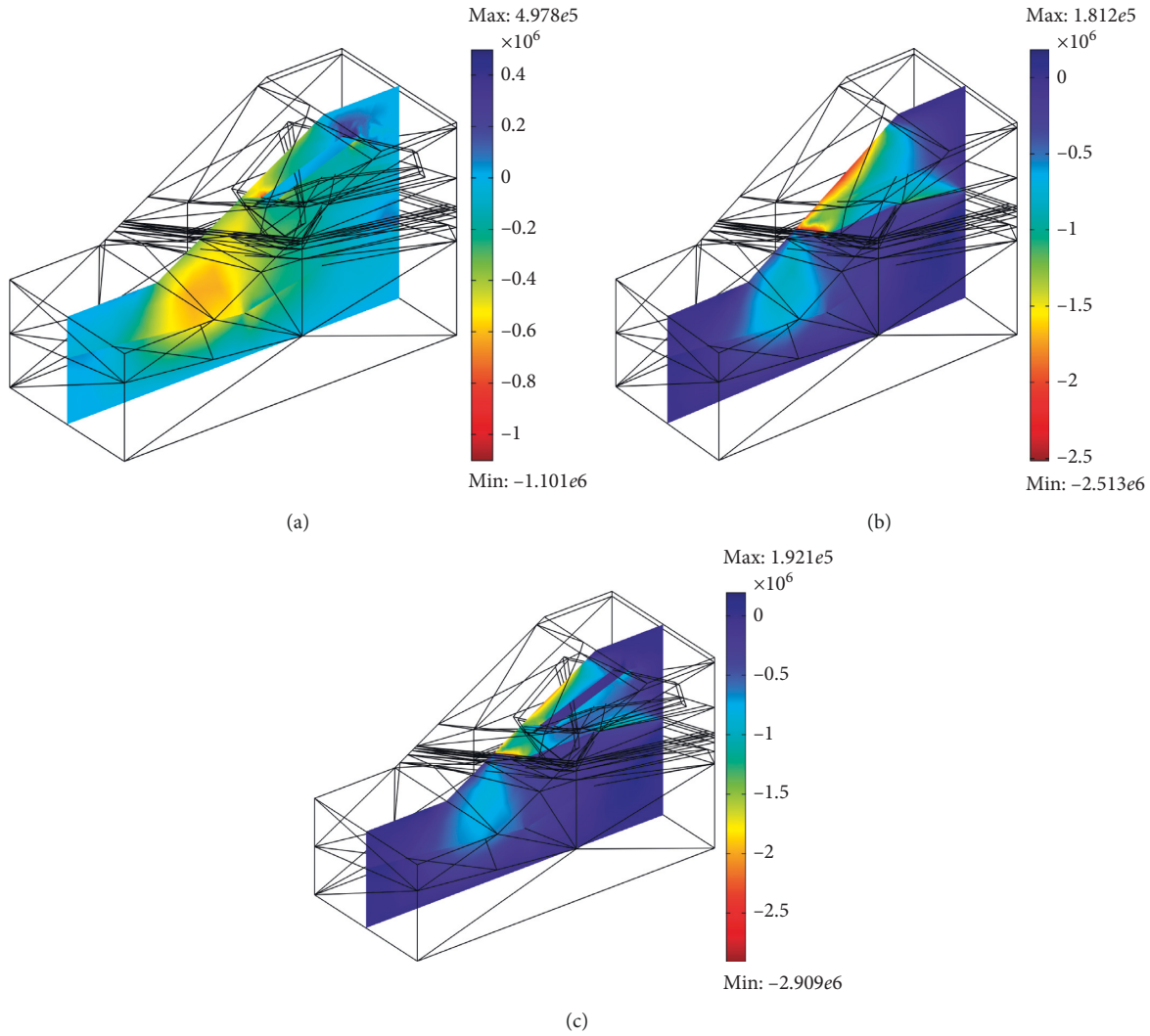

Figure 17: Shear stress field under three conditions. (a) Only fault. (b) Only weak layer. (c) Both fault and weak layer.

shear stress on the xz plane under three conditions. It can be seen that the changes of shear stress of the slope with fault are the smallest, and the changes of shear stress of the slope with both fault and weak layer are the largest and the most complicated. The maximum value of shear stress is 0.57 MPa when the slope contains only fault, 2.49 MPa when it contains only weak layer, and 2.70 MPa when it contains both fault and weak layer. At the fault and weak layer, the abnormal changes of the curves are caused, which indicates that the fault and weak layer cause the

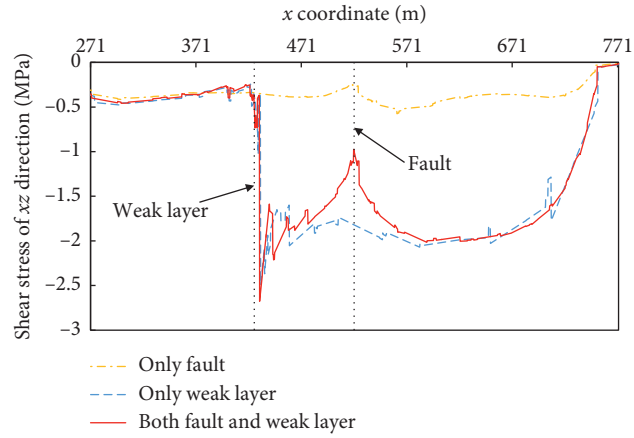

Figure 18: Changes of shear stress field under three conditions.

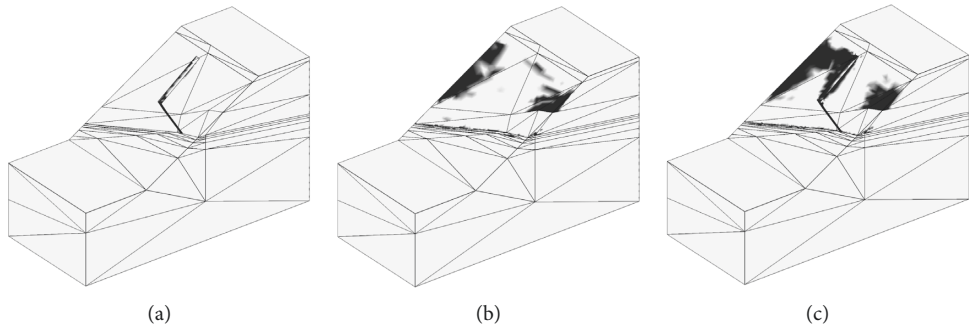

Figure 19: Damage zone under three conditions when $F = 1.3$. (a) Only fault. (b) Only weak layer. (c) Both fault and weak layer.

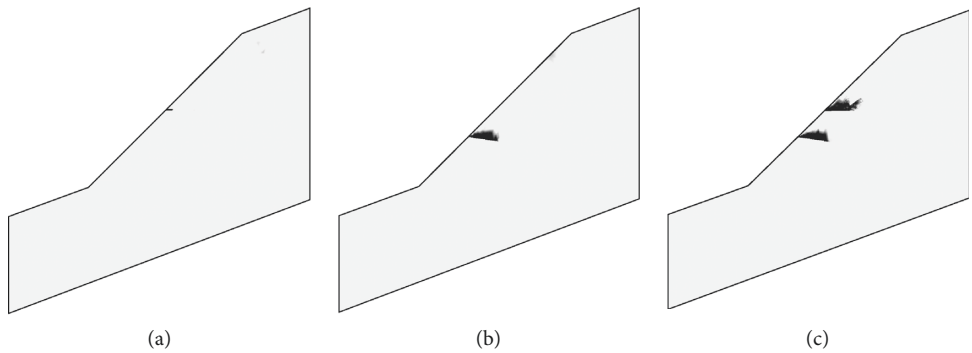

Figure 20: Sectional view of the damage zone under three conditions when $F = 1.3$. (a) Only fault. (b) Only weak layer. (c) Both fault and weak layer.

stress concentration in the slope. And the stress change caused by the weak layer is much higher than that caused by the fault.

6.3.2. Comparative Analysis of Damage Evolution. Figures 19 and 20 are comparisons of the damage zone under the three conditions when $F = 1.3$. Among them, the damage zone of the slope with fault is the smallest. Damage only occurs at the fault, and the depth of the damage zone is not large. The damage zone of the slope with weak layer is larger. Damage occurs not only at the weak layer, but also on the slope above the weak layer. The depth of the damage zone is larger. The damage zone of the slope with fault and weak layer is the largest. Besides fault and weak layer, damage also occurs on the slope surface on both sides of the fault and above the weak layer. The depth of the damage zone is the largest.

According to the degree of effect on slope stability, the condition of the slope with fault and weak layer has the greatest effect on the stability of the slope, the condition of the slope with weak layer is the second, and the condition of

the slope with fault is least. The fault and weak layer have different degrees of effect on the slope stability. The fault causes stress concentration and damage to nearby rock mass. The weak layer causes stress concentration on the slope above it and forms a dangerous slip zone. This is related to the occurrence of fault and weak layer in the slope. Whether it is a fault or a weak layer, it can be regarded as a structural surface that affects the stability of the slope. When the structural surface and the slope surface are nearly vertical, the structural surface has little effect on the stability of the slope. When the structural surface is nearly parallel to the slope surface, the structural surface has a great effect on the slope stability and may cause instability. In the slope model of this paper, the fault is the structural surface in the vertical direction, and the weak layer is the structural surface in the horizontal direction. Therefore, the weak layer has a greater effect on the slope stability than the fault.

7. Conclusions

In this paper, taking complex 3D slope as the research object, the stress field and damage evolution law of the slope under three conditions are analyzed by using COMSOL numerical calculation software and FESRM. The main conclusions are as follows:

(1) For the condition of the slope with fault and weak layer, the slope stability is obviously affected. According to the analysis results, the fault and weak layer have different degrees of effect on the slope stability. The fault causes stress concentration and damage to nearby rock mass. The weak layer causes stress concentration on the slope above it and forms a dangerous slip zone. Under the effect of the fault and weak layer, stress concentration occurs in the rock mass near the fault and weak layer, which makes the surrounding rock mass more vulnerable to damage, and makes the slope extremely easy to landslide instability.

(2) For the condition of the slope with only fault, the slope stability is not affected much. The fault causes stress concentration on both sides of it and damage to surrounding rock mass. For the condition of the slope with only weak layer, the effect of slope stability is obvious. The weak layer causes the stress concentration on the slope above it and forms a slip zone, which makes the slope easy to landslide. Compared with the effect of the weak layer, the fault has little effect on the stability of the slope.

(3) According to the degree of effect on slope stability, the condition of the slope with fault and weak layer has the greatest effect on the stability of the slope, the condition of the slope with weak layer is the second, and the condition of the slope with fault is least. This is related to the occurrence of fault and weak layer in the slope. Because the effect of horizontal structural plane on slope stability is greater than that of vertical structural plane, the effect of weak layer on slope stability is greater than that of the fault in the slope model of this paper.

Abbreviations

ρ: Density
c: Cohesion before strength reduction
φ: Internal friction angle before strength reduction
E: Elastic modulus
μ: Poisson's ratio
c': Cohesion after strength reduction
φ': Internal friction angle after strength reduction
F: Strength reduction factor
I_1: First invariant of stress
J_2: Second invariant of stress deviator
σ_1: Maximum principal stress
σ_2: Intermediate principal stress
σ_3: Minimum principal stress
σ_x: Normal stress in the x direction
σ_y: Normal stress in the y direction
σ_z: Normal stress the in z direction
τ_{xy}: Shear stress on the xy plane
τ_{yz}: Shear stress on the yz plane
τ_{zx}: Shear stress on the zx plane
α,K: Experimental constants related only to φ and c.

Data Availability

The data used to support the findings of this study are included within the article.

Conflicts of Interest

The authors declare that there are no conflicts of interest regarding the publication of this paper.

Acknowledgments

The authors sincerely thank the kind assistance provided by Dr. Wenhao Shi. The authors gratefully acknowledge the support from China Postdoctoral Science Foundation (2018M641200), Fundamental Research Funds for the Central Universities (FRF-TP-18-021A1), and National Key R&D Program of China (2017YFC0602901).

References

[1] S. W. Sloan, "Geotechnical stability analysis," *Géotechnique*, vol. 63, no. 7, pp. 531–571, 2013.

[2] S. Leroueil, "Natural slopes and cuts: movement and failure mechanisms," *Géotechnique*, vol. 51, no. 3, pp. 197–243, 2001.

[3] D. V. Griffiths and R. M. Marquez, "Three-dimensional slope stability analysis by elasto-plastic finite elements," *Géotechnique*, vol. 57, no. 6, pp. 537–546, 2007.

[4] S.-Y. Zhao, Y.-R. Zhen, W.-M. Shi, and J.-L. Wang, "Analysis on safety factor of slope by strength reduction FEM," *Chinese Journal of Geotechnical Engineering*, vol. 24, no. 3, pp. 343–346, 2002.

[5] L.-Y. Zhang, Y.-R. Zheng, S.-Y. Zhao, and W.-M. Shi, "Feasibility study of strength-reduction method with fem for

calculating safety factors of soil slope stability," *Journal of Hydraulic Engineering*, vol. 34, no. 1, pp. 21–27, 2003.

[6] M.-W. Guo, C.-G. Li, and S.-L. Wang, "Three-Dimensional slope stability analysis based on finiteelement stress," *Chinese Journal of Rock Mechanics and Engineering*, vol. 31, no. 12, pp. 122–128, 2012.

[7] S.-Y. Zhao, Y.-R. Zhen, and W.-D. Deng, "Stability analysis on jointed rock slope by strength reduction fem," *Chinese Journal of Rock Mechanics and Engineering*, vol. 22, no. 2, pp. 254–260, 2003.

[8] Y.-S. Lin and S.-H. Chen, "Search of three-dimensional slip surface for slope based onfinite element calculation," *Rock and Soil Mechanics*, vol. 34, no. 4, pp. 1191–1196, 2013.

[9] D.-P. Deng and L. Li, "Limit equilibrium analysis of slope stability with coupling nonlinear strength criterion and double-strength reduction technique," *International Journal of Geomechanics*, vol. 19, no. 6, pp. 1–13, 2019.

[10] J.-X. Ma, Z.-S. Lai, Q.-E. Cai, and Z.-L. Xu, "3D Fem analysis of slope stability based on strength reduction method," *Chinese Journal of Rock Mechanics and Engineering*, vol. 23, no. 16, pp. 2690–2693, 2004.

[11] L.-D. Wei, C.-H. Yang, and C.-S. Gao, "Optimization of slide-resistant piles based on strength reduction method with 3D FEM," *Chinese Journal of Geotechnical Engineering*, vol. 27, no. 11, pp. 1350–1352, 2005.

[12] T.-K. Nian, K.-L. Zhang, and H.-Y. Xu, "Stability and faliure mechansim of three-dimensional slope using strength reduction method," *Journal of Jilin University (Earth Science Edition)*, vol. 1, pp. 181–188, 2013.

[13] O. C. Zienkiewicz, C. Humpheson, and R. W. Lewis, "Associated and non-associated visco-plasticity and plasticity in soil mechanics," *Géotechnique*, vol. 25, no. 4, pp. 671–689, 1975.

[14] K. Ugai, "A method of calculation of total safety factor of slope by elasto-plastic FEM," *Soils and Foundations*, vol. 29, no. 2, pp. 190–195, 1989.

[15] D. V. Griffiths and P. A. Lane, "Slope stability analysis by finite elements," *Géotechnique*, vol. 49, no. 3, pp. 387–403, 1999.

[16] E. M. Dawson, W. H. Roth, and A. Drescher, "Slope stability analysis by strength reduction," *Géotechnique*, vol. 49, no. 6, pp. 835–840, 1999.

[17] M. T. Manzari and M. A. Nour, "Significance of soil dilatancy in slope stability analysis," *Journal of Geotechnical and Geoenvironmental Engineering*, vol. 126, no. 1, pp. 75–80, 2000.

[18] F. Tschuchnigg, H. F. Schweiger, and S. W. Sloan, "Slope stability analysis by means of finite element limit analysis and finite element strength reduction techniques. part I: numerical studies considering non-associated plasticity," *Computers and Geotechnics*, vol. 70, pp. 169–177, 2015.

[19] Z.-Y. Lian, G.-C. Han, and X.-J. Kong, "Study on stability of excavated slope by strength reduction finite element method," *Chinese Journal of Geotechnical Engineering*, vol. 23, no. 4, pp. 407–411, 2001.

[20] Y.-R. Zhen, S.-Y. Zhao, and L.-Y. Zhang, "Slope stability analysis by finite element strength reduction method," *Strategic Study of CAE*, vol. 4, no. 10, pp. 57–78, 2002.

[21] L.-H. Chen and X.-G. Jin, "Applicability of three failure criteria for slope in finite element strength reduction method," *China Civil Engineering Journal*, vol. 45, no. 9, pp. 136–146, 2012.

[22] S.-Y. Zhao, Y.-R. Zhen, and Y.-F. Zhang, "Lecture on finite element method for limit analysis ii discussion on criteria of slope instability in finite element strength reduction method," *Rock and Soil Mechanics*, vol. 26, no. 2, pp. 332–336, 2005.

[23] L.-J. Pei, B.-N. Qu, and S.-G. Qian, "Uniformity of slope instability criteria for finite element strength reduction method," *Rock and Soil Mechanics*, vol. 31, no. 10, pp. 3337–3341, 2010.

[24] Y.-F. Zhou, J.-H. Deng, Y.-L. Cui, H.-C. Zheng, and T. Chen, "Instability criterion of three-dimensional slope based on strength reduction method," *Rock and Soil Mechanics*, vol. 35, no. 5, pp. 1430–1437, 2014.

[25] W. Yuan, X.-C. Li, W. Wang, B. Bai, Q.-Z. Wang, and X.-J. Chen, "A study of strength reduction method with double reduction coefficient," *Rock and Soil Mechanics*, vol. 37, no. 8, pp. 2222–2230, 2016.

[26] Z.-L. Song, T. Yang, and L.-C. Zhao, "Contrastive analysis of stability evaluation methods for progressive rock slopes containing multilayer weak interlayers," *The Chinese Journal of Geological Hazard and Control*, vol. 27, no. 2, pp. 20–25, 2016.

[27] Z. T. Bieniawski, "The rock mass rating (rmr) system (geomechanics classification) in engineering practice," in *Symposium on Rock Classification Systems for Engineering Purposes*, L. Kirkaldie, Ed., pp. 17–34, Cincinnati, OH, USA, 1988.

[28] E. Hoek and E. T. Brown, *Underground Excavations in Rock*, Institution of Mining and Metallurgy, London, UK, 1980.

[29] E. Hoek and E. T. Brown, "Empirical strength criterion for rock masses," *Journal of the Geotechnical Engineering Division, ASCE*, vol. 106, no. 9, pp. 1013–1035, 1980.

[30] E. Hoek and E. T. Brown, "The Hoek-Brown failure criterion—a 1988 update," in *Proceedings of the 15th Canadian Rock Mechanics Symposium*, J. H. Curran, Ed., pp. 31–38, Civil Engineering Dept., University of Toronto, Toronto, Canada, 1988.

[31] E. Hoek, D. Wood, and S. Shah, "A modified Hoek-Brown criterion for jointed rock masses," in *Proceedings of the Rock Characterization, Symposium of ISRM: Eurock 92*, J. Hudson, Ed., pp. 209–213, British Geotechnical Society, London, UK, 1992.

[32] Y.-R. Zhen, S.-Y. Zhao, and Y.-K. Song, "Advance of study on the strength reduction finite element method," *Journal of Logistical Engineering University*, vol. 21, no. 3, pp. 1–6, 2005.

[33] M.-F. Cai, M.-C. He, and D.-Y. Liu, *Rock Mechanics and Engineering*, Science Press, Beijing, China, 2002.

[34] A. M. Naji, M. Z. Emad, H. Rehman, and H. Yoo, "Geological and geomechanical heterogeneity in deep hydropower tunnels: a rock burst failure case study," *Tunnelling and Underground Space Technology*, vol. 84, no. 2, pp. 507–521, 2019.

[35] A. M. Naji, H. Rehman, M. Z. Emad, and H. Yoo, "Impact of shear zone on rockburst in the deep neelum-jehlum hydropower tunnel: a numerical modeling approach," *Energies*, vol. 11, no. 8, 1935 pages, 2018.